doi: 10.56761/EFRE2024.C1-P-023104

Multichannel injection of hydrogen in a pulsed plasma accelerator

V.E. Zavalova[*], *A.A. Kozlov, A.V. Kozlov, V.P. Polistchook, Yu.V. Karpushin, M.A. Shurupov*

Joint Institute for High Temperatures of RAS, Moscow, Russia
[*]*zavalova@fites.ru*

Abstract. The multichannel hydrogen injection (MHI) system, which is the initial section of a pulsed plasma accelerator (PPA), has been described. MHI was provided synchronous hydrogen supply through the six electrodynamics valves. Hydrogen ionization has been started after the breakdown of the discharge gap, to which the voltage of ~25 kV from a capacitive storage device was applied. The geometry of plasma formation (PF) was greatly influenced by the external pulsed magnetic field, which was created in the initial section of PPA. The diagnostic system included measurement of the electrical characteristics of the discharge (Rogowski coils and voltage dividers), temperature and electron density (Langmuir triple probe, spectral methods), optical visualization of the plasma shell motion with a time resolution of about 2 μs. The dynamic of the hydrogen pressure increasing was estimated by the breakdown voltage of the model gap. The stages of arising and development of PF in the MHI has been investigated.
Keywords: hydrogen injection, pulsed plasma accelerator of coaxial type, plasma formation.

1. Introduction

Pulsed plasma accelerators (PPA) are used to generate high-speed plasma jets to solve various scientific and applied problems. Similar jets can be formed in accelerators with pulsed filling of the working gas. For example, they may be used in the guns that "shoot" plasma clots in a rarefied environment [1], or in thermonuclear fusion installations [2]. For practical application, high-energy plasma clots or plasma formations (PF) weighing over 20 mg and energy content over 100 kJ are required. In this work, a multichannel hydrogen injection (MHI) system has been tested, with the help of which it is expected to increase the mass and energy content of the PF in PPA.

2. Description of the experimental setup and diagnostic methods

Fig. 1 presents the design of the MHI system, which is the initial section of the PPA. The following notations are used: 1 – external electrode (anode), 2 – insulator with a developed surface to prevent breakdown along it, 3 – electrodynamic gas valve (GV), 4 – wire for powering the GV, 5 – terminals for powering the external solenoid, 6 – fiberglass bandage, 7 – internal electrode (cathode), 8 – socket with a bracket for installing diagnostic probes, 9 – flange/viewing window with a Wilson seal and a device for inserting probes, 10 – external solenoid, 11 – gas mixer, 12 – current collector. The installation parts had the following dimensions: anode diameter – 150 mm, cathode diameter – 70 mm, distance from the gas mixer to the inspection window – 366 mm. The volume of the MHI was ~ 8l. The cathode has a concave surface, which contributes to the swirling of the gas jet coming from the valves. The design of the electro-dynamic valve has been described in [3, 4].

The voltage to the discharge part was supplied from capacitive storage device CSD1 (charging voltage up to 50 kV, capacity – 12 μF). CSD1 was applied to initiate breakdown of the inter-electrode gap and obtain initial PF. A solid-state discharger (SSD) [3], which has a low parasitic inductance, was used for battery switching. An external magnetic field was created by a solenoid, which has been powered from a CSD2 (charging voltage up to 40 kV, capacity – 96 μF). The solenoid was made of a copper busbar, the internal diameter of the solenoid was 150 mm, length was 83 mm, the number of turns was 3, and the number of starts was 4.

Before the experiment the pressure in the MHI was ~ 0.1 mPa. The start of the switchers, the supply of gas through the six GVs into the discharge gap, and the start of the SSD for its breakdown were synchronized in accordance with certain delay times associated with different speeds of

operation of the valves. According to estimates, under the nominal operating mode of one GV, ~10 mg of hydrogen entered the PPA.

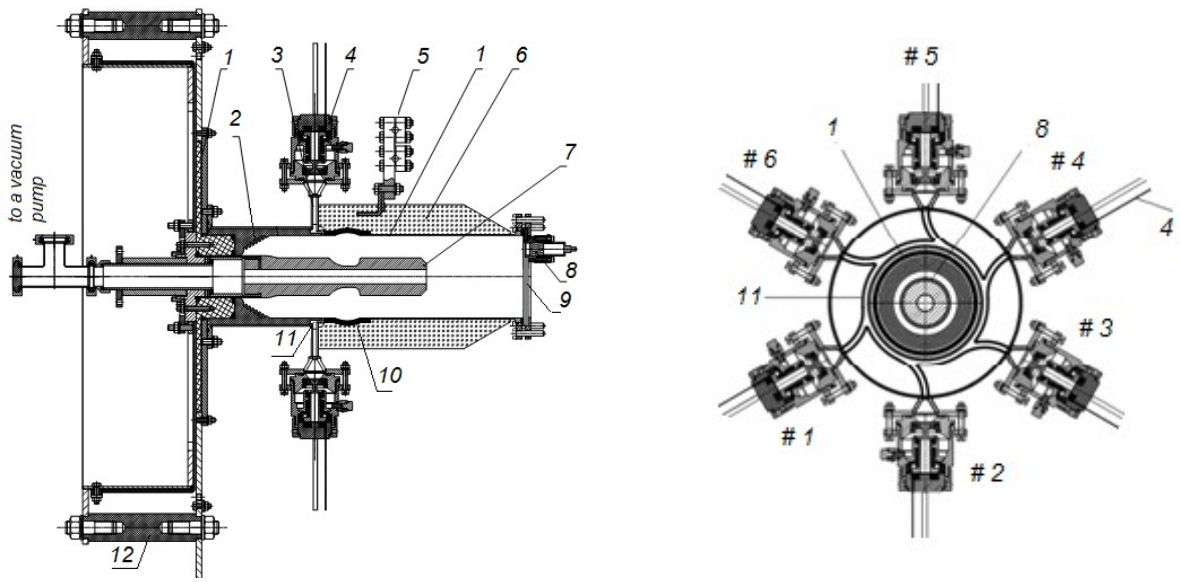

Fig. 1. Design of a multi-channel injection system, longitudinal and cross-sectional views.

The currents in the discharge gap and solenoid were determined with help of the Rogowski coils, and the discharge voltage was measured using a voltage divider. Plasma parameters were estimated from known relationships [5, 6]: electron temperature was obtained from the intensity's ratio of the H_α and H_β lines of the hydrogen atom of the Ballmer series, electron concentration was determined from the H_β line broadening. The M266 monochromator (Solar-Company) was used for spectral diagnostics. An adapter attachment was installed on the output flange of the MHI to input radiation through an optical fiber into the monochromator. The electron temperature was estimated by the intensity ratio method for lines H_α ($\lambda = 656$ nm) and H_β ($\lambda = 486$ nm). For this purpose, a grating of 300 lines/mm was installed in the monochromator. A diffraction grating of 1200 lines/mm was used to estimate the electron concentration n_e. The hardware broadening was 0.063 nm.

The electron temperature and density were also estimated using by the three-point Langmuir probe according to the method described in [7]. The three-point probe consisted of three insulated molybdenum wires with the diameter of 0.5 mm and the length of 15 mm, which were introduced into the plasma flow through the MHI flange at a distance from 120 to 355 mm from it. The discharge was recorded using a Phantom-VEO-710 high-speed camera; characteristic shooting mode: spatial resolution 64×64 pixels, shooting speed — 430000 frames per second, exposure time was ~ 2 μs.

The hydrogen concentration n_a in the MHI was estimated by the breakdown voltage V_b of the probe gap; breakdown occurred after the valve was activation at various points in time depending on the applied voltage. Copper electrodes of the breakdown probe (BP) with the spherical ends were spaced at a distance of $d_p = 6$ mm from each other. PB was inserted into the chamber through socket 7 (Fig. 1). After the voltage V_b from 2 to 8 kV was applied to BP, the GV was triggered and the time of breakdown occurrence was fixed. According to the Paschen criterion, gap breakdown occurs when an electron, "knocked out" by ions from the cathode, on its way to the anode creates the same number of ions that ensured its escape from the cathode [8]. This is possible when a sufficient number of hydrogen molecules are supplied from the injector in the discharge gap. The

drift velocity of electrons (1) u_e and their current density $j_e = n_e u_e$ (2) in a flat gap are found from the equations [8]:

$$u_e = \frac{eE}{m_e k_e n_a}, \quad (1)$$

$$\frac{dj_e}{dx} = k_i n_e n_a \quad (2)$$

Where E is the electric field intensity, e and me are the charge and mass of the electron, k_e and k_i are the constant of elastic collisions of electrons with molecules and their ionization constant respectively. There is no ion current at the anode surface, while the electron current at the cathode surface is proportional to the ion current: $j_e = -\gamma j_i$. The distribution of electrons over the gap can be obtained taking into account these boundary conditions, and then the analytical expression for the Paschen criterion may be written as (3):

$$eV_b \ln\left(1 + {}^1/_\gamma\right) = m_e k_e k_i n_a^2 d_p^2 \quad (3)$$

The collision constants k_e and k_i depend on the Townsend parameter E/n_a. The drift velocity of electrons and their temperature T_e depended on this parameter were taken from the reference book [9]. The constant k_i was calculated under the assumption that ionization occurs by direct electron impact from the ground state of the hydrogen molecule and that the ionization cross section is proportional to the difference between the electron energy and the ionization potential [8]; the proportionality coefficient was equal to $6 \cdot 10^{-18}$ cm^2/eV [9]. The ion-electron emission coefficient γ for a proton is approximately ~0.1 [8]. The hydrogen concentration at different times after the activation of the GV was determined from the relation (3) by the value of breakdown voltage.

3. Experimental results

Fig. 2 shows oscillograms of current and voltage in the discharge; the charging voltage of CSD1 was 25 kV, the cathode-anode distance was 40 mm. This figure also shows the solenoid current (I_s) at CSD2 charging voltage of 10 kV.

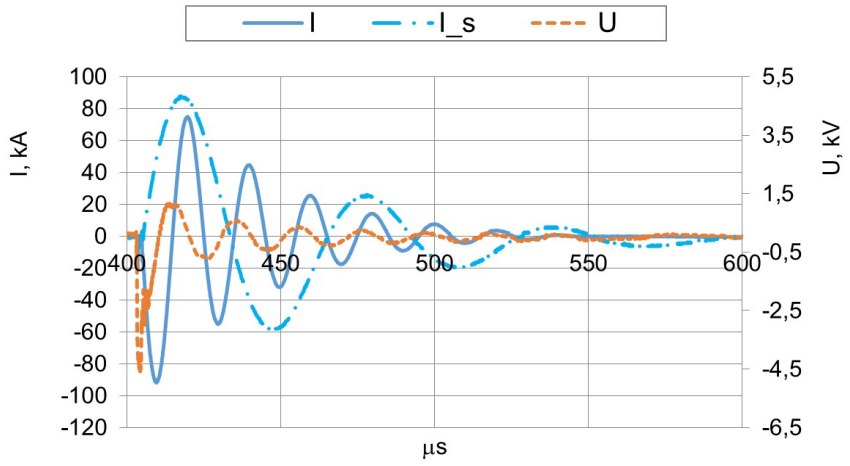

Fig. 2. Oscillograms of current I and voltage U in the discharge gap and solenoid current I_s.

The estimated induction of magnetic field at the maximum current in the solenoid in the discharge gap, without taking into account the shielding of the camera body, was about of 2 T. The maximum discharge current was about of 90 kA, the period of oscillations of the damped current was about 20 microseconds; the maximum current in the solenoid was ~90 kA, its period was ~ 60 μs.

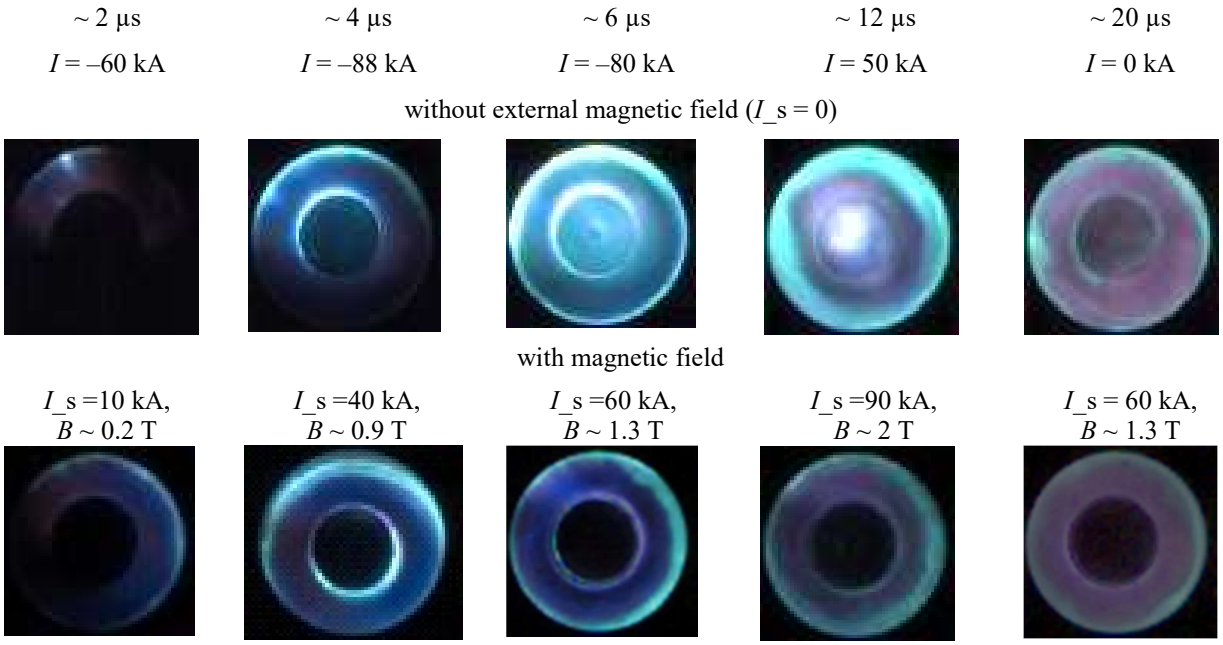

Fig. 3. Frames of the formation and decay of a PF without a magnetic field (top) and with the magnetic field of an external solenoid powered by a voltage of ~10 kV.

Analysis of the obtained images (Fig. 3) in accordance with the oscillograms in Fig. 2 showed that the establishment time of PF after the the breakdown was about 5–6 μs, which corresponded to a quarter of the current period. Without an external magnetic field the plasma expanded beyond the shorter internal electrode, and for another half period of the current (10 μs) the glow was bright, then the glow gradually decreased, and it was not registered at all until about 100 μs (discharge current decay). When the solenoid was turned on, the PF glow stopped much earlier, at 80 μs. In this case, the PF retained a ring shape with clear boundaries along the electrodes, but under these conditions we did not observe the release of plasma into the region in front of the internal electrode. Increasing the charging voltage CSD2 from 10 to 14 kV did not change the overall picture of the obtained images, while the magnetic field intensity was enlarged significantly. This feature is expected to be studied in more detail in the future.

Analysis of the data on the time of development of the breakdown of BP (d_p = 6 mm) showed that the breakdown when pumping gas from one valve at a probe voltage of 8 kV occurred after 0.58 ms and developed within ~1.4 μs. When a voltage of 5 kV was applied to the probe, a breakdown occurred at 0.62 ms and developed for ~0.8 μs. At 2 kV, the breakdown occurred at 0.65 ms and developed for 0.6 μs. Thus, the breakdown voltage of the discharge gap lay on the left branch of the Paschen curve [8]. Relation (3) is valid for the right branch of this curve and near its minimum, when the mean free path of electrons is small compared to the interelectrode gap. Therefore, relation (3) can only be used for the experiment with a breakdown voltage of 2 kV; in this mode, the calculated value of the hydrogen density from relation (3) was $5 \cdot 10^{16}$ cm^{-3}. It can be assumed that the rate of hydrogen inflow into the MGI was approximately constant, therefore, the breakdown which occured at 400 μs after the valve opening at voltage of 25 kV, corresponded to a hydrogen concentration of ~ $3 \cdot 10^{16}$ cm^3. During the discharge combustion time (~ 0.1 ms), the hydrogen concentration in the MGI increased by ~20%.

The plasma radiation spectrum is presented in Fig. 4. Estimates of the electron temperature in the discharge gave the value T_e = 1.4 eV, which corresponds to the average temperature in the interelectrode gap during the exposure time. The characteristic value of the half-width of the H_β line

taking into account the hardware broadening was $\Delta\lambda_{1/2} \sim 1.2$ nm. The average width of line H_β corresponded to the value $n_e \sim 1.5 \cdot 10^{14}$ cm^{-3}.

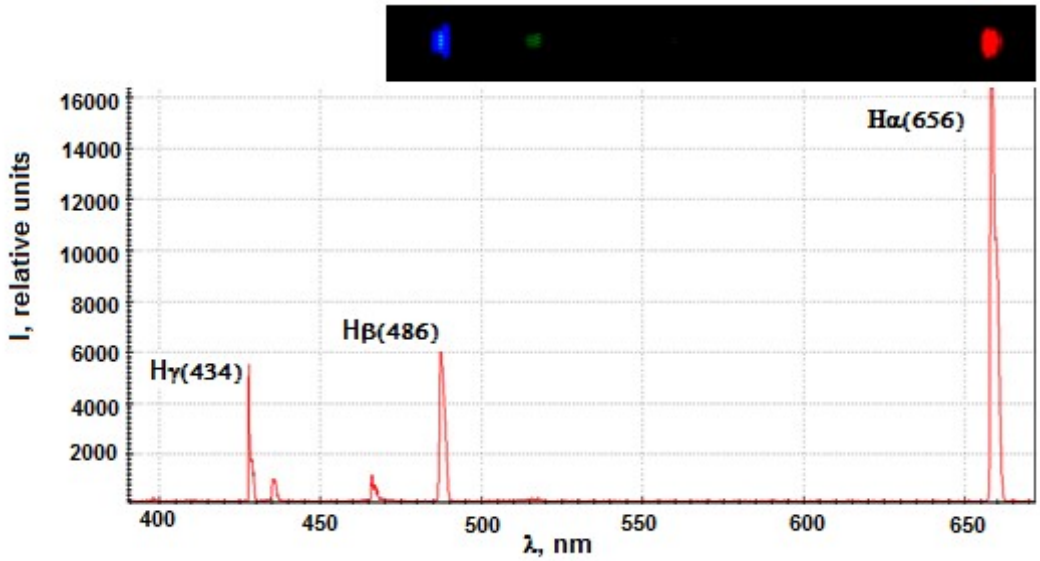

Fig. 4. The spectrum taken by the matrix of the Phonton VEO-710 camera (top), and the corresponding distribution of the spectrum of atomic hydrogen of the Balmer series, produced by the monochromator (from the built-in Toshiba camera).

The values of electron concentration and temperature obtained from Langmuir probe data are presented in Fig. 5. The main ranges of electron temperature and density were 1÷3 eV and $5 \cdot 10^{14} \div 2 \cdot 10^{15}$ cm^{-3}, respectively.

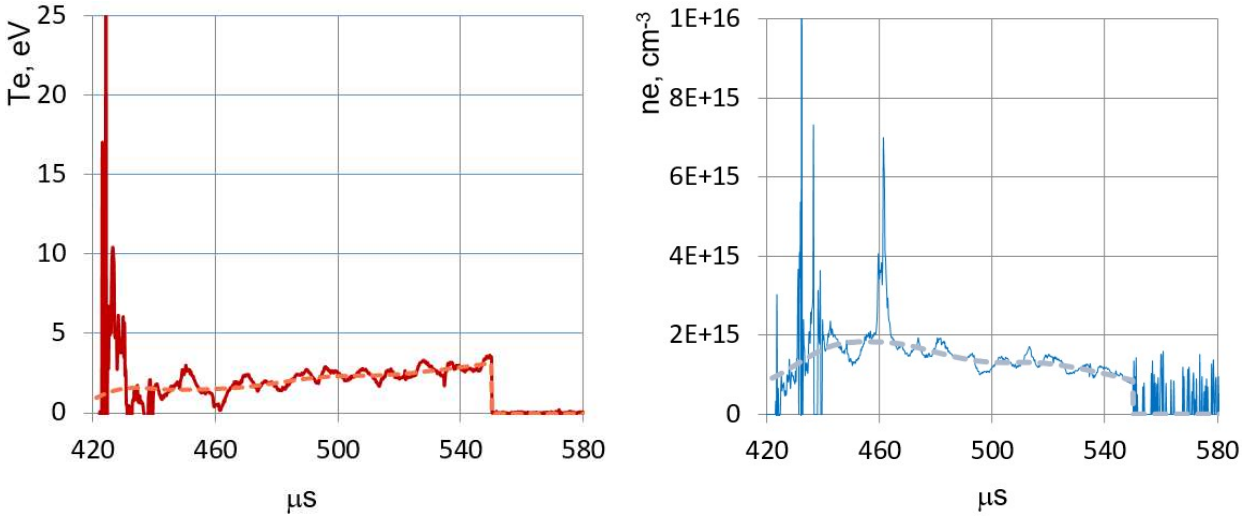

Fig. 5. Electron temperature T_e and density n_e with averaging (dotted lines).

As can be seen, the averaged values agree satisfactorily with the spectral measurements. In the case of probe measurements, changes in values during the pulse can be monitored. The use of a triple Langmuir probe has additional advantages. Firstly, the measurements are local in nature and the position of the probe in the interelectrode space can be changed. Secondly, the three-point probe makes it possible to determine simultaneously the electron temperature and estimate the local electron density in the plasma.

4. Conclusion

The design features of the working gas multichannel injection system, which is the initial section of a PPA, have been described. The diagnostics of the main characteristics of plasma formation has been enlarged: it included measurements of the electrical characteristics of the installation; energy characteristics of the plasma flow, both by the spectral method and using a triple Langmuir probe. A technique for estimation of pulsed gas pressure during plasma formation was proposed and tested. The developed system is shown to be promising for use in PPA to increase the mass and energy content of the plasma flow.

5. References

[1] S.G. Bannov, A.M. Zhitlukhin, V.E. Cherkovets, E.L. Stupitsky, A.A. Motorin, A.S. Kholodov, Dynamics of the Plasma Bunch at the Initial and Following Stages of Motion in a Rarefied Gas, *Geomagnetism and Aeronomy*, vol. **59**, 318, 2019, doi: 10.1134/S0016793219030034

[2] V.V. Gavrilov, A.G. Eskov, A.M. Zhitlukhin, D.M. Kochnev, I.M. Poznyak, D.A. Toporkov, N.M. Umrikhin, S.A. Pikuz, S.N. Ryazantsev, I.Y. Skobelev, Counter Collision of High-Energy Plasma Flows in a Longitudinal Magnetic Field, *Plasma Physics Reports,* vol. **46**, 689, 2020, doi: 10.1134/S1063780X20070041

[3] D.A. Toporkov, D.A. Burmistrov, K.V. Zhuravlev, S.D. Lidzhigoryaev, V.A. Kostyushin, I.M. Poznyak, R.R. Usmanov, V.Yu. Tsybenko and V.S. Nemchinov, MK-200, *Plasma Gun Facility. Instrum Exp Tech*, vol. **66**, 920, 2023, doi: 10.1134/S0020441223050111

[4] A.N. Gusev, A.V. Kozlov, A.V. Shurupov, A.V. Mashtakov and M.A. Shurupov, A Solid-State Discharger for a High-Current Energy Source Based on a Capacitive Storage with an Operating Voltage of 50 kV, *Instrum Exp Tech*, vol. **63**, 58, 2020, doi: 10.1134/S0020441220010133

[5] S.V. Polosatkin, E.S. Grishnyaev, V.I. Davydenko, I.A. Ivanov, A.A. Podyminogin, I.V. Shikhovtsev, Optical spectroscopy of plasma of the radio-frequency emitter of a powerful fast neutral beam injector, *Instrum Exp Tech,* vol. **53**, 253, 2010, doi: 10.1134/S002044121002017X

[6] W. Lochte-Holtgreven, *Plasma diagnostics*. Amsterdam: North-Holland Pub. Co. 1968.

[7] S. Borthakur, N. Talukdar, N. K. Neog, and T. K. Borthakur, Study of plasma parameters in a pulsed plasma accelerator using triple Langmuir probe, *Physics of plasma*, vol. **25**, 013532, 2018, doi: 10.1063/1.5009796

[8] Yu.P. Raizer, *Gas Discharge Physics*. Springer, 1997.

[9] I.S. Grigoriev, E.Z. Meilikhov (Eds.), *Physical quantities*. *Handbook*, *[in Russian]*. Moscow: Energoatomizdat, 1991.